Asymptotically Tight Performance Bounds for Equal-Gain Combining Over a New Correlated Fading Channel

Adebola Olutayo, *Student Member, IEEE*, Julian Cheng, *Senior Member, IEEE*, Jonathan Holzman, *Member, IEEE*

***Abstract*—A recently proposed fading model which can be used to describe both line-of-sight and non-line-of-sight components of a fading channel is analyzed. The outage probability and error rate performance of equal-gain combining over arbitrary correlated Beaulieu-Xie fading channels is considered. Asymptotically-tight closed-form lower and upper bounds are derived and these analytical results are verified via Monte Carlo simulations.**

I. Introduction

Wireless systems with both line-of-sight (LOS) signal and multi-path (non-LOS) signals have been largely characterized by the Ricean fading model. However, the Ricean fading lacks the flexibility to model different fading severity because of its unity diversity order [1]. To overcome the challenges of inadaptability of the Ricean fading to fading variations, the Nakagami-m fading model was proposed which has a flexible fading parameter, m. However, it has been concluded that the Nakagami-m fading model, which can be derived from the central Chi-distribution, is only suitable for systems with multi-path (non-LOS) signals [2]-[4].

A recently proposed fading model, which we refer to as the Beaulieu-Xie fading model in this work, was derived from the non-central Chi-distribution. This fading model acquires the advantages of the Ricean and Nakagami-m fading models, through its ability to model both LOS signals and multi-path (non-LOS) signals and flexibility to model various fading severity which is enabled by its flexible fading parameter, m. The Beaulieu-Xie fading model is a normalized form of the non-central Chi-distribution as the Nakagami-m fading model is a normalised form of the central Chi-distribution. This new fading model has been shown to have a relationship with the generalized Ricean distribution and the $\kappa - \mu$ distribution [1], which makes the performance analysis of this fading model to be of utmost importance. To the best of the authors' knowledge, there has been no performance analysis reported beyond the works in [5] and [6].

Diversity technique is of enormous importance in radio communications in the presence of co-channel interference and multipath fading. Diversity combining schemes play a vital role in limiting these undesirable effects on transmitted signals. There is generally an assumption of independence when considering spatial diversity; however, this is most often not the case. For example, in large multiple-input-multiple-output implementations, this assumption of independence is only valid when there is sufficient spacing among receiving branches [7]. We will therefore consider correlated Beaulieu-Xie fading channels in this paper for equal-gain combining (EGC). EGC is considered because it has simpler implementation than maximal ratio combining (MRC), but EGC performs closely to optimal MRC [8]-[10].

This work makes the following major contributions. Asymptotically tight closed-form error rate and outage probability bounds at high signal-to-noise (SNR) are developed and analysed for EGC over arbitrarily correlated Beaulieu-Xie channels. The performance of EGC diversity reception over arbitrarily correlated and independent Beaulieu-Xie fading channels is analysed.

II. System Model

Linear diversity reception with N branches operating over the Beaulieu-Xie fading model is considered here. The received signal is obtained as

$$\mathbf{y} = \mathbf{z}x + \mathbf{n} \tag{1}$$

where x is the transmitted signal, $\mathbf{n}$ is a random vector denoting additive Gaussian white noise (AWGN), and $\mathbf{z}$ is the fading channel vector, i.e., the real fading amplitude. In addition, $\mathbf{z} = [z_1, \ldots, z_N]^T = [\sqrt{\bar{\gamma}_1}Z_1, \ldots, \sqrt{\bar{\gamma}_N}Z_N]^T$, where $[\cdot]^T$ represents the transpose, $\bar{\gamma}_n$ is the average received SNR of the nth branch, and Z_n is the fading amplitude of the nth branch. The output SNR for EGC diversity reception is given as

$$\gamma_{EGC} = \frac{1}{N}\left(\sum_{n=1}^{N} z_n\right)^2. \tag{2}$$

The Beaulieu-Xie fading amplitude associated with the nth branch is

$$Z_n = \sqrt{\sum_{i=1}^{2m} X_{n,i}^2}; \quad \forall n = 1, \ldots N \tag{3}$$

where $X_{n,i}$,$\forall i = 1, \ldots 2m$ are Gaussian RVs with mean μ, variance $\left(\frac{1}{2m}\right)$ and m is a half-integer, representing the fading parameter that controls the shape of the probability density function (pdf) of the fading model. The nth component of $\mathbf{z}$ can be obtained by generating $N \times 2m$ matrix of Gaussian RVs, $\mathbf{B}$, whose entries are $b_{n,i}$ whose mth column is denoted as $\mathbf{b}_m$, such that $\mathbf{B} = (\mathbf{b}_1, \ldots, \mathbf{b}_{2m})$. We obtain the vector, $\mathbf{b} = \left[\mathbf{b}_1^T, \ldots, \mathbf{b}_{2m}^T\right]^T = [b_{1,1}, b_{2,1}, \ldots, b_{n,2m}]^T$. We can, therefore, express the fading amplitude over the nth branch as

$$z_n = \sqrt{\sum_{i=1}^{2m} b_{n,i}^2}; \quad \forall n = 1, \ldots N. \tag{4}$$

The pdf of $\mathbf{b}$ is expressed as

$$f_{\mathbf{b}}(\mathbf{b}) = \frac{1}{\sqrt{(2\pi)^{2mN}|\mathbf{R_b}|}} \times \exp\left(-\frac{1}{2}(\mathbf{b}-\boldsymbol{\mu_b})^T\mathbf{R_b}^{-1}(\mathbf{b}-\boldsymbol{\mu_b})\right) \quad (5)$$

where $\boldsymbol{\mu_b}$ is the $2mN \times 1$ mean vector and $\mathbf{R_b}$ is the $2mN \times 2mN$ covariance matrix of $\mathbf{b}$. The determinant of the covariance matrix $\mathbf{R_b}$ is expressed in terms of the correlation matrix $\mathbf{C_b}$ by [10]

$$|\mathbf{R_b}| = \frac{\left(\prod_{n=1}^{N}\bar{\gamma}_n^{2m}\right)|\mathbf{C_b}|}{(2m)^{2mN}}.$$

This new fading model has a diversity order mN, similar to the Nakagami-m fading model. For the same value of m, but the former has improved performance due to its inclusion of the LOS component [1].

III. Relationship between the Power correlation and Gaussian Correlation Coefficient

We employ the Cholesky decomposition to define the correlation between RVs $X_{n,i}$ and $X_{j,k}$ with mean μ and variance $\frac{1}{2m}$ [8]. It can be shown that $X_{n,i} = \rho_{(n,i)(j,k)}X_{j,k} + \sqrt{1-\rho^2_{(n,i)(j,k)}}W$ with mean zero and variance $\frac{1}{2m}$, and it is independent of $X_{j,k}$. The relationship between the correlation coefficient of the Gaussian RVs and the power correlation coefficient is

$$\rho_{z^2_{n_1}z^2_{n_2}} = \frac{K-(2m)^2T^2}{(2+2m)U-(2m)^2T^2} \quad (6)$$

where $K = \sum_{i=1}^{2m}\sum_{k=1}^{2m}\left(3U^2\rho^2_{(n,i)(j,k)} + T^2\left(1-\rho^2_{(n,i)(j,k)}\right)\right)$, $T = \frac{1}{2m}+\mu^2$, and $U = \frac{1}{2m}$.

IV. Bounds on the pdf

The pdf of $\mathbf{b}$ shall be bounded in the region $\mathbf{b}^T\mathbf{b} \le r^2$, which is a $2mN$-dimensional sphere with radius r. This is achieved by considering the exponential component of (5). Applying the Rayleigh quotient as $R_y\left(\mathbf{R_b}^{-1},\mathbf{b}\right) = \frac{\mathbf{b}^T\mathbf{R_b}^{-1}\mathbf{b}}{\mathbf{b}^T\mathbf{b}}$, where $\mathbf{R_b}$ is a positive definite matrix. The range of R_y is obtained as $\lambda_{\min} \le \frac{\mathbf{b}^T\mathbf{R_b}^{-1}\mathbf{b}}{\mathbf{b}^T\mathbf{b}} \le \lambda_{\max}$, such that $\lambda_i \ge 0$, $\lambda_{\min}$ and $\lambda_{\max}$ are the smallest and largest eigenvalues of $\mathbf{R_b}^{-1}$, respectively. Thus, when $\lambda_{\min} = 0$ we have

$$0 \le \mathbf{b}^T\mathbf{R_b}^{-1}\mathbf{b} \le \lambda_{\max}\mathbf{b}^T\mathbf{b}. \quad (7)$$

Further expansion of the exponential component leads to

$$(\mathbf{b}-\boldsymbol{\mu_b})^T\mathbf{R_b}^{-1}(\mathbf{b}-\boldsymbol{\mu_b}) = \mathbf{b^T}\mathbf{R_b}^{-1}\mathbf{b} + \boldsymbol{\mu_b}^T\mathbf{R_b}^{-1}\boldsymbol{\mu_b} + 2\left|\boldsymbol{\mu_b}^T\mathbf{R_b}^{-1}\mathbf{b}\right|, \quad (8)$$

where we assume that $\mathbf{R_b}^{-1^T} = \mathbf{R_b}^{-1}$.

Using the 2-norm of the matrix as $\|\mathbf{b}\| = \sqrt{\mathbf{b^T}\mathbf{b}} = \sqrt{r}$, such that (8) becomes

$$-2\left\|\boldsymbol{\mu_b}^T\mathbf{R_b}^{-1}\right\|\sqrt{r} \le (\mathbf{b}-\boldsymbol{\mu_b})^T\mathbf{R_b}^{-1}(\mathbf{b}-\boldsymbol{\mu_b}) \le \lambda_{max}r + 2\left\|\boldsymbol{\mu_b}^T\mathbf{R_b}^{-1}\right\|\sqrt{r}. \quad (9)$$

The upper and lower bounds of the pdf are then obtained as

$$f_{\mathbf{b}}(\mathbf{0})\exp\left(-\frac{1}{2}\left(\lambda_{max}r + 2\left\|\boldsymbol{\mu_b}^T\mathbf{R_b}^{-1}\right\|\sqrt{r}\right)\right) \le f_{\mathbf{b}}(\mathbf{b}) \le f_{\mathbf{b}}(\mathbf{0})\exp\left(\left\|\boldsymbol{\mu_b}^T\mathbf{R_b}^{-1}\right\|\sqrt{r}\right). \quad (10)$$

V. Performance Bounds of EGC

A. Outage Probability Bounds on EGC

We express the outage probability for EGC with respect to a signal threshold, γ_{th}, as

$$P_o^{EGC}(\gamma_{th}) = \Pr\{\gamma_{\mathrm{EGC}} \le \gamma_{\mathrm{th}}\}. \quad (11)$$

Substituting (3) into (2b) and then substituting the result into (11) give

$$P_o^{EGC}(\gamma_{th}) = \Pr\left\{\frac{1}{N}\left(\sum\nolimits_{n=1}^{N}\sqrt{\sum\nolimits_{i=1}^{2m}b^2_{n,i}}\right)^2 \le \gamma_{th}\right\} = \int_{\gamma_{EGC}\le\gamma_{th}} f_{\mathbf{b}}(\mathbf{b})d\mathbf{b}. \quad (12)$$

1) Asymptotic Outage Probability Approximation of EGC: The asymptotic outage probability approximation is obtained by substituting $f_{\mathbf{b}}(\mathbf{b}) \approx f_{\mathbf{b}}(\mathbf{0})$ in (12) to give

$$P_{o,\infty}^{EGC}(\gamma_{th}) = f_{\mathbf{b}}(\mathbf{0})\int_{\gamma_{EGC}\le\gamma_{th}} d\mathbf{b} \quad (13)$$

where $\gamma_{EGC} = \frac{1}{N}\left(\sum_{n=1}^{N}\sqrt{\sum_{i=1}^{2m}b^2_{n,i}}\right)^2$. The integral in (13) is obtained as [8]

$$\int_{\gamma_{EGC}\le\gamma_{th}} d\mathbf{b} = \left(\frac{2m\pi^m}{\Gamma(m+1)}\right)^N\frac{\Gamma^N(2m)}{(2mN)}(N\gamma_{th})^{mN}. \quad (14)$$

Equation (14) is substituted into (13) to give the asymptotic outage probability approximation as

$$P_{o,\infty}^{EGC}(\gamma_{th}) = f_{\mathbf{b}}(\mathbf{0})\left(\frac{2m\pi^m}{\Gamma(m+1)}\right)^N\frac{\Gamma^N(2m)}{(2mN)}(N\gamma_{th})^{mN}. \quad (15)$$

2) Lower Bound Outage Probability of EGC: The lower bound of the outage probability bound is obtained by replacing $f_{\mathbf{b}}(\mathbf{0})$ in (13) with the lower bound of $f_{\mathbf{b}}(\mathbf{b})$ in (10) to give

$$P_{o,LB}^{EGC}(\gamma_{th}) = O_{LB}\times\int_{\gamma_{EGC}\le\gamma_{th}} d\mathbf{b} \quad (16)$$

where $O_{LB} = f_{\mathbf{b}}(\mathbf{0})\exp\left(-\frac{1}{2}\left(\lambda_{max}N\gamma_{th} + 2\left\|\mu_{\mathbf{b}}{}^T\mathbf{R_b}^{-1}\right\|\sqrt{N\gamma_{th}}\right)\right)$. Substituting the result of the integral in (14) into (16) gives the lower bound of the outage probability as

$$P_{o,LB}^{EGC}(\gamma_{th}) = O_{LB}\times\left(\frac{2m\pi^m}{\Gamma(m+1)}\right)^N\frac{\Gamma^N(2m)}{(2mN)}(N\gamma_{th})^{mN}. \quad (17)$$

3) Upper Bound on Outage Probability of EGC: The upper bound outage of the probability bound is obtained by replacing $f_{\mathbf{b}}(\mathbf{0})$ in (13) by the upper bound of $f_{\mathbf{b}}(\mathbf{b})$ in (10), and one

obtains

$$P_{o,UB}^{EGC}(\gamma_{th}) = O_{UB} \times \int\limits_{\gamma_{EGC} \leq \gamma_{th}} d\mathbf{b} \tag{18}$$

where $O_{UB} = f_{\mathbf{b}}(\mathbf{0}) \exp\left(\left\|{\boldsymbol{\mu}_{\mathbf{b}}}^T \mathbf{R}_{\mathbf{b}}^{-1}\right\| \sqrt{N\gamma_{th}}\right)$. Substituting the result of the integral in (14) into (18) gives the upper bound of the outage probability as

$$P_{o,UB}^{EGC}(\gamma_{th}) = O_{UE} \times \left(\frac{2m\pi^m}{\Gamma(m+1)}\right)^N \frac{\Gamma^N(2m)}{(2mN)} (N\gamma_{th})^{mN}. \tag{19}$$

VI. Performance Bounds of Error Rate

A. Error Rate Bounds on EGC

The error rate for EGC is expressed as

$$\begin{aligned} P_e^{EGC} &= E\left[pQ\left(\sqrt{\frac{q}{N}\left(\sum_{n=1}^{N}\sqrt{\sum_{i=1}^{2m} b_{n,i}^2}\right)^2}\right)\right] \\ &= p\int\limits_{-\infty}^{\infty} Q\left(\sqrt{\frac{q}{N}\left(\sum_{n=1}^{N}\sqrt{\sum_{i=1}^{2m} b_{n,i}^2}\right)^2}\right) f_{\mathbf{b}}(\mathbf{b})\, d\mathbf{b}. \end{aligned} \tag{20}$$

where $E[\cdot]$ denotes the expectation operation, and the Gaussian Q-function is $Q(x) = \frac{1}{\sqrt{2\pi}} \int\limits_{x}^{\infty} \exp\left(\frac{-t^2}{2}\right) dt$. For the special case of coherent binary phase shift keying (BPSK), we have $p = 1$ and $q = 2$.

1) Asymptotic Error Rate Approximation of EGC: The asymptotic error rate approximation is obtained by substituting $f_{\mathbf{b}}(\mathbf{b}) \approx f_{\mathbf{b}}(\mathbf{0})$ in (20) to give

$$P_{e,\infty}^{EGC} = p f_{\mathbf{b}}(\mathbf{0}) \int\limits_{-\infty}^{\infty} Q\left(\sqrt{\frac{q}{N}\left(\sum_{n=1}^{N}\sqrt{\sum_{i=1}^{2m} b_{n,i}^2}\right)^2}\right) d\mathbf{b} \tag{21}$$

where we obtain the integral in (21) according to [10 eq. (61)]. This is simplified to give

$$P_{e,\infty}^{EGC} = p f_{\mathbf{b}}(\mathbf{0}) \times G(R_{th}) \tag{22}$$

where

$$\begin{aligned} G(R_{th}) &= \left(\frac{2m\pi^m}{\Gamma(m+1)}\right)^N \left(\frac{\Gamma^N(2m)}{\Gamma(2mN)}\right) \\ &\times \left(\frac{N^{mN} 2^{mN-2}}{\sqrt{\pi} mN q^{mN}} \Gamma\left(mN + \frac{1}{2}\right)\right). \end{aligned} \tag{23}$$

2) Lower Error Rate Bound of EGC: The lower bound of the error rate is obtained by changing the integral bound in (21) as

$$P_e^{EGC} = p \int\limits_{R_{EGC} \leq R_{th}^2} Q\left(\sqrt{\frac{q}{N}\left(\sum_{n=1}^{N}\sqrt{\sum_{i=1}^{2m} b_{n,i}^2}\right)^2}\right) f_{\mathbf{b}}(\mathbf{b})\, d\mathbf{b} \tag{24}$$

where $R_{EGC} = \sqrt{\frac{q}{N}\left(\sum_{n=1}^{N}\sqrt{\sum_{i=1}^{2m} b_{n,i}^2}\right)^2}$. Substituting $f_{\mathbf{b}}(\mathbf{b})$ with the lower bound of $f_{\mathbf{b}}(\mathbf{b})$ in (10) into (24), and we simplify to have

$$P_{e,LB}^{EGC} = p f_{\mathbf{b}}(\mathbf{0}) \times E_{LB} \times Y(R_{th}) \tag{25}$$

where

$$\begin{aligned} E_{LB} = f_{\mathbf{b}}(\mathbf{0}) \exp\Bigg(&-\frac{1}{2}\left(\lambda_{\max} N {R_{th}}^2\right. \\ &\left.+2\left\|{\mu_{\mathbf{b}}}^T \mathbf{R}_{\mathbf{b}}^{-1}\right\| \sqrt{N} R_{th}\right)\Bigg) \end{aligned} \tag{26}$$

and

$$\begin{aligned} Y(R_{th}) = &\left(\frac{2m\pi^m}{\Gamma(m+1)}\right)^N \left(\frac{\Gamma^N(2m)}{\Gamma(2mN)}\right) \left[\left(\frac{2^{mN-2} N^{mN}}{\sqrt{\pi} mN q^{mN}}\right.\right. \\ &\left.\left. \times\ \gamma\left(mN + \frac{1}{2}, \frac{q}{2}{R_{th}}^2\right) + Q\left(\sqrt{q} R_{th}\right) \frac{{R_{th}}^{2mN} N^{mN}}{2mN}\right)\right], \end{aligned} \tag{27}$$

where $\gamma(\cdot,\cdot)$ is the incomplete gamma function as, $\gamma(\alpha, x) = \int\limits_{0}^{x} e^{-t} t^{\alpha-1} dt$ [10].

3) Upper Error Rate Bound of EGC: The upper error rate bound is obtained by splitting the integral region in (21) according to

$$\begin{aligned} &P_{e,UB}^{EGC} \\ &= p \int\limits_{R_{EGC} \leq R_{th}^2} Q\left(\sqrt{\frac{q}{N}\left(\sum_{n=1}^{N}\sqrt{\sum_{i=1}^{2m} b_{n,i}^2}\right)^2}\right) f_{\mathbf{b}}(\mathbf{b}) d\mathbf{b} \\ &+ p \int\limits_{R_{EGC} > R_{th}^2} Q\left(\sqrt{\frac{q}{N}\left(\sum_{n=1}^{N}\sqrt{\sum_{i=1}^{2m} b_{n,i}^2}\right)^2}\right) f_{\mathbf{b}}(\mathbf{b})\, d\mathbf{b}. \end{aligned} \tag{28}$$

We substitute $f_{\mathbf{b}}(\mathbf{b})$ with the upper bound of $f_{\mathbf{b}}(\mathbf{b})$ in (10) for the first part, and $f_{\mathbf{b}}(\mathbf{b})$ with $f_{\mathbf{b}}(\boldsymbol{\mu}_{\mathbf{b}})$, which is the largest value of $f_{\mathbf{b}}(\mathbf{b})$ for the second part. This gives

$$\begin{aligned} &P_{e,UB}^{EGC} \\ &= p \times E_{UE} \times \int\limits_{R_{EGC} \leq R_{th}^2} Q\left(\sqrt{q\sum_{n=1}^{N}\sum_{i=1}^{2m} b_{n,i}^2}\right) d\mathbf{b} \\ &+ p f_{\mathbf{b}}(\boldsymbol{\mu}_{\mathbf{b}}) \underbrace{\int\limits_{R_{EGC} > R_{th}^2} Q\left(\sqrt{\frac{q}{N}\left(\sum_{n=1}^{N}\sqrt{\sum_{i=1}^{2m} b_{n,i}^2}\right)^2}\right) d\mathbf{b}}_{I(\boldsymbol{\mu}_{\mathbf{b}})} \end{aligned} \tag{29}$$

where $E_{UB} = f_{\mathbf{b}}(\mathbf{0}) \exp\left(\left\|{\boldsymbol{\mu}_{\mathbf{b}}}^T \mathbf{R}_{\mathbf{b}}^{-1}\right\| \sqrt{N} R_{th}\right)$. The first integral in (29) is simplified according to (27), and the second integral is simplified as (30) on top of the next page. We show some mathematical manipulations in (31) and (32) to further

$$I\left(\boldsymbol{\mu}_{\mathbf{b}}\right)=\int_{-\infty}^{\infty}\left(\sqrt{\frac{q}{N}\left(\sum_{n=1}^{N}\sqrt{\sum_{i=1}^{2m}b_{n,i}^{2}}\right)^{2}}\right)d\mathbf{b}-\int_{R_{EGC}\leq R_{th}^{2}}Q\left(\sqrt{\frac{q}{N}\left(\sum_{n=1}^{N}\sqrt{\sum_{i=1}^{2m}b_{n,i}^{2}}\right)^{2}}\right)d\mathbf{b}. \tag{30}$$

$$\int_{R_{EGC}\leq R_{th}^{2}}Q\left(\sqrt{\frac{q}{N}\left(\sum_{n=1}^{N}\sqrt{\sum_{i=1}^{2m}b_{n,i}^{2}}\right)^{2}}\right)d\mathbf{b}\geq\int_{R_{EGC}\leq R_{th}^{2}}Q\left(\sqrt{q\sum_{n=1}^{N}\sum_{i=1}^{2m}b_{n,i}^{2}}\right)d\mathbf{b}, \tag{31}$$

$$=\int_{-\infty}^{\infty}Q\left(\sqrt{\frac{q}{N}\left(\sum_{n=1}^{N}\sqrt{\sum_{i=1}^{2m}b_{n,i}^{2}}\right)^{2}}\right)d\mathbf{b}-\int_{R_{EGC}\leq R_{th}^{2}}Q\left(\sqrt{q\sum_{n=1}^{N}\sum_{i=1}^{2m}b_{n,i}^{2}}\right)d\mathbf{b} \tag{32}$$

simplify (30) on top of the next page. Ultimately, we express (30) as

$$Z(R_{th})=G(R_{th})-\frac{\pi^{mN}}{\Gamma\left(mN+1\right)}\left[R_{th}^{2mN}Q\left(\sqrt{q}R_{th}\right)+\frac{2^{mN-1}}{\sqrt{\pi}q^{mN}}\gamma\left(mN+\frac{1}{2},\frac{q}{2}R_{th}^{2}\right)\right]. \tag{33}$$

Substituting (27) and (33) into (29) gives the error rate upper bound.

VII. Discussion on the Tightness of Bounds

A. Tightness of the Outage Probability Bound

We show the tightness of the bounds on the outage probability analytically by considering the lower and upper bounds in (17) and (19), respectively. The difference between the expression of the asymptotic approximation, lower and upper bounds is seen in the exponential component. An increase in the average SNR per branch by a factor P, yields an increase in the covariance matrix $\mathbf{R_b}$ by a factor P, which eventually leads to a decrease in $\mathbf{R_b}^{-1}$ by the same factor. The eigenvalues of $\mathbf{R_b}^{-1}$ will also be affected by the same factor P. We, therefore, obtain the limit of the ratio of the lower bound to the upper bound as P tends to infinity as

$$\lim_{P\to\infty}=\frac{P_{o,LB}}{P_{o,UB}}=\frac{\exp\left(-\frac{1}{2}\left(\frac{\lambda_{max}\gamma_{th}}{P}+2\left\|\frac{\mu_{\mathbf{b}}^{T}\mathbf{R_b}^{-1}}{P}\right\|\sqrt{\gamma_{th}}\right)\right)}{\exp\left(\left\|\frac{\mu_{\mathbf{b}}^{T}\mathbf{R_b}^{-1}}{P}\right\|\sqrt{\gamma_{th}}\right)}.$$

The above limit shows that the bounds of the outage probability will converge to the asymptotic approximation as SNR approaches infinity.

B. Tightness of the Error Rate Bound

By definition, the incomplete gamma function is expressed as

$$\Gamma\left(s\right)=\lim_{x\to\infty}\gamma\left(s,x\right) \tag{34}$$

and the Chernoff bound of the Q-function

$$Q\left(x\right)\leq e^{-\frac{x^{2}}{2}},\quad x>0. \tag{35}$$

We apply these definitions to $Y(R_{th})$ and $Z(R_{th})$ in (27) and (33), respectively, to show the tightness of the error rate bounds, according to

$$\lim_{R_{th}\to\infty}Y=G(R_{th}) \tag{36}$$

$$\lim_{R_{th}\to\infty}Z=G-\frac{\pi^{mN-\frac{1}{2}}}{\Gamma\left(mN+1\right)}\left[\frac{2^{mN-1}}{q^{mN}}\Gamma\left(mN+\frac{1}{2}\right)\right]. \tag{37}$$

We consider the exponential component, where we observe that an increase in the average SNR per branch by a factor K results in an increase in the covariance matrix $\mathbf{R_b}$, leading to a decrease in $\mathbf{R_b}^{-1}$, which eventually leads to a decrease in λ_{max} by the same factor K. Thus, the limit is found to be

$$\lim_{K\to\infty}=\frac{P_{e,LB}}{P_{e,UB}}=\frac{\exp\left(-\frac{1}{2}\left(\frac{\lambda_{max}K}{K}+2\left\|\frac{\mu_{\mathbf{b}}^{T}\mathbf{R_b}^{-1}}{K}\right\|\sqrt{K}\right)\right)}{\exp\left(\left\|\frac{\mu_{\mathbf{b}}^{T}\mathbf{R_b}^{-1}}{K}\right\|\sqrt{K}\right)} \tag{38}$$

where R_{th} is expressed in terms of K, i.e., $R_{th}=\sqrt{K}$.

VIII. Numerical Results

Figure 1 shows a comparison of outage probability curves of EGC for a 2-branch diversity system over correlated and independent Beaulieu-Xie fading channels with coherent BPSK modulation and a fading parameter of $m=1.5$. Correlation structure of the form $\mathbf{C_b}=[\mathbf{C}_1,\mathbf{0}_{2\times2},\mathbf{0}_{2\times2};\mathbf{0}_{2\times2},\mathbf{C}_2,\mathbf{0}_{2\times2};\ \mathbf{0}_{2\times2},\mathbf{0}_{2\times2},\mathbf{C}_3]$, where $\mathbf{C}_1=\mathbf{C}_2=\mathbf{C}_3=\left[1,\sqrt{0.35};\sqrt{0.35},1\right]$ and $\mathbf{C}_1=\mathbf{C}_2=\mathbf{C}_3=[1,0;0,1]$, is considered for correlation and independence, respectively. The independent channels outperform the correlated channels. The effect of correlation is seen on the rate of convergence of the bounds in both scenarios.

Figure 2 shows a comparison of BER curves EGC for a 2-branch diversity system over correlated and independent Beaulieu-Xie fading channels with coherent BPSK modulation and a fading parameter of $m=1.5$. Correlation matrix of the form $\mathbf{C_b}=[\mathbf{C}_1,\mathbf{0}_{2\times2},\mathbf{0}_{2\times2};\mathbf{0}_{2\times2},\mathbf{C}_2,\mathbf{0}_{2\times2};\mathbf{0}_{2\times2},\mathbf{0}_{2\times2},\mathbf{C}_3]$ is considered, where $\mathbf{C}_1=\mathbf{C}_2=\mathbf{C}_3=\left[1,\sqrt{0.3};\sqrt{0.3},1\right]$ and $\mathbf{C}_1=\mathbf{C}_2=\mathbf{C}_3=[1,0;0,1]$ are considered for correlation and independence, respectively. The effect of correlation is shown on the rate of convergence of the bounds.

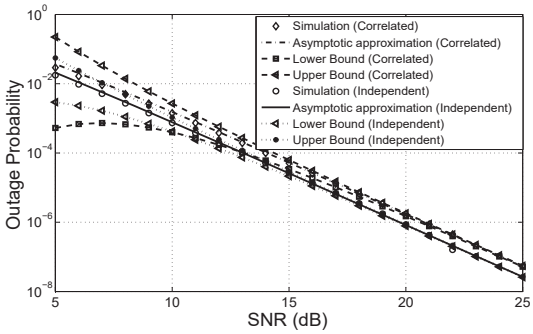

Fig. 1. Outage probability curves for the asymptotic approximation, lower bound, and upper bound for MRC over correlated and independent Beaulieu-Xie fading channels. The number of branches is N = 2, the fading parameter is m = 1.5, and the correlation structure is $\mathbf{C_b} = [\mathbf{C}_1, \mathbf{0}_{2\times2}, \mathbf{0}_{2\times2}; \mathbf{0}_{2\times2}, \mathbf{C}_2, \mathbf{0}_{2\times2}; \mathbf{0}_{2\times2}, \mathbf{0}_{2\times2}, \mathbf{C}_3]$, where $\mathbf{C}_1 = \mathbf{C}_2 = \mathbf{C}_3 = \left[1, \sqrt{0.35}; \sqrt{0.35}, 1\right]$ and $\mathbf{C}_1 = \mathbf{C}_2 = \mathbf{C}_3 = [1, 0; 0, 1]$ are for correlation and independence, respectively.

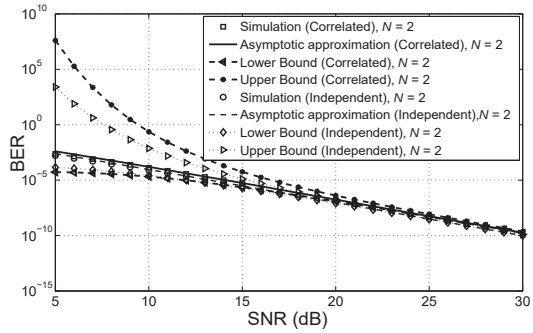

Fig. 2. BER curves for the asymptotic approximation, lower bound, and upper bound for EGC, over correlated and independent Beaulieu-Xie fading channels. The number of branches is N = 2, the fading parameter is m = 1.5, and the correlation structure is $\mathbf{C_b} = [\mathbf{C}_1, \mathbf{0}_{2\times2}, \mathbf{0}_{2\times2}; \mathbf{0}_{2\times2}, \mathbf{C}_2, \mathbf{0}_{2\times2}; \mathbf{0}_{2\times2}, \mathbf{0}_{2\times2}, \mathbf{C}_3]$, where $\mathbf{C}_1 = \mathbf{C}_2 = \mathbf{C}_3 = \left[1, \sqrt{0.3}; \sqrt{0.3}, 1\right]$ and $\mathbf{C}_1 = \mathbf{C}_2 = \mathbf{C}_3 = [1, 0; 0, 1]$ are for correlation and independence, respectively.

Figure 3 shows a comparison of BER curves EGC for a 2- and 3- branch diversity systems over correlated and independent Beaulieu-Xie fading channels with coherent BPSK modulation and a fading parameter of $m = 1.5$. The correlation structure for the 2-branch system is of the form $\mathbf{C_b} = [\mathbf{C}_1, \mathbf{0}_{2\times2}, \mathbf{0}_{2\times2};\ \ \mathbf{0}_{2\times2}, \mathbf{C}_2, \mathbf{0}_{2\times2}; \mathbf{0}_{2\times2}, \mathbf{0}_{2\times2}, \mathbf{C}_3]$, where $\mathbf{C}_1 = \mathbf{C}_2 = \mathbf{C}_3 = \left[1, \sqrt{0.3}; \sqrt{0.3}, 1\right]$ and for the 3-branch system is of the form $\mathbf{C_b} = [\mathbf{C}_1, \mathbf{0}_{3\times3}, \mathbf{0}_{3\times3}; \mathbf{0}_{3\times3}, \mathbf{C}_2, \mathbf{0}_{3\times3}; \mathbf{0}_{3\times3}, \mathbf{0}_{3\times3}, \mathbf{C}_3]$, where $\mathbf{C}_1 = \mathbf{C}_2 = \mathbf{C}_3 = \left[1, \sqrt{0.3}, \sqrt{0.15}; \sqrt{0.3}, 1, \sqrt{0.3}; \sqrt{0.15}, \sqrt{0.3}, 1\right]$. The effect of diversity is shown here; the performance for the 3-branch system is improved over the 2-branch system.

IX. Conclusion

We derived asymptotically tight lower and upper bounds for outage probability and error rate for the new Beaulieu-Xie fading. The presence of more than one LOS component is seen (analytically) on the performance of the model by the means of the exponent component of the Gaussian pdf. We have shown the effect of correlation and independence on the performance of the system and also the effect of the number of branches of the diversity system. We can conclude

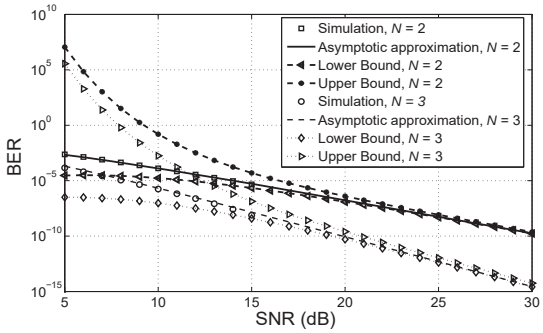

Fig. 3. Comparison of BER curves for the asymptotic approximation, lower bound, and upper bound for EGC for 2- and 3-branch diversity systems over correlated Beaulieu-Xie fading channels. The fading parameter is m = 1.5. The correlation structure for the 2-branch system is $\mathbf{C_b} = [\mathbf{C}_1, \mathbf{0}_{2\times2}, \mathbf{0}_{2\times2};\ \ \mathbf{0}_{2\times2}, \mathbf{C}_2, \mathbf{0}_{2\times2}; \mathbf{0}_{2\times2}, \mathbf{0}_{2\times2}, \mathbf{C}_3]$, where $\mathbf{C}_1 = \mathbf{C}_2 = \mathbf{C}_3 = \left[1, \sqrt{0.3}; \sqrt{0.3}, 1\right]$, and for the 3-branch system is $\mathbf{C_b} = [\mathbf{C}_1, \mathbf{0}_{3\times3}, \mathbf{0}_{3\times3}; \mathbf{0}_{3\times3}, \mathbf{C}_2, \mathbf{0}_{3\times3}; \mathbf{0}_{3\times3}, \mathbf{0}_{3\times3}, \mathbf{C}_3]$, where $\mathbf{C}_1 = \mathbf{C}_2 = \mathbf{C}_3 = \left[1, \sqrt{0.3}, \sqrt{0.15}; \sqrt{0.3}, 1, \sqrt{0.3}; \sqrt{0.15}, \sqrt{0.3}, 1\right]$.

that this new fading model can be effective in characterizing wireless communication links with both LOS and non-LOS components.

References

[1] N. C. Beaulieu and J. Xie, "A novel fading model in channel with multiple dominant specular components," *IEEE Wireless Commun. Lett.*, vol. 4, no. 1, pp. 54-57, Feb. 2015.

[2] M. D. Yacoub, "Nakagami-m phase-envelope joint distribution: A new model," *IEEE Trans. Veh. Technol.*, vol. 59, no. 3, pp. 1552-1557, Mar. 2010.

[3] N. C. Beaulieu and S. A. Saberali, "A generalized diffuse scatter plus line-of-sight fading channel model," in *Proc. IEEE ICC 2014*, Sydney, NSW, Jun., 2014, pp. 5849-5853.

[4] S. Wyne, A. P. Singh, F. Tufvesson, and A. F. Molisch, "A statistical model for indoor office wireless sensor channels," *IEEE Trans. Wireless Commun.*, vol. 8, no. 8, pp. 4154-4164, Aug. 2009.

[5] A. Olutayo, J. Cheng and J. F. Holzman, "Asymptotically tight performance bounds for selection combining over new fading channels with arbitrary correlation," *Proc. IEEE ICC 2017*, Paris, Jun., 2017.

[6] A. Olutayo, H. Ma, J. Cheng and J. F. Holzman, "Level crossing rate and average fade duration for a new fading model," *IEEE Wireless Commun. Lett.*: submitted, Feb., 2017.

[7] M. Schwartz, W. R. Bennett, and S. Stein, *Communication Systems and Techniques*, New York: McGraw-Hill, 1996.

[8] V. V. Veeravalli, "On performance analysis for signaling on correlated fading channels," *IEEE Trans. Commun.*, vol. 49, no. 11, pp. 1879-1883, Nov. 2001.

[9] V. A. Aalo, "Performance of maximal-ratio diversity systems in a correlated Nakagami-fading environment," *IEEE Trans. Commun.*, vol. 43, no. 8, pp. 2360-2369, Aug. 1995.

[10] B. Zhu F. Yang, J. Cheng, and L. Wu, "Performance bounds for diversity receptions over arbitrarily correlated Nakagami-m fading channel," *IEEE Trans. Wireless Commun.*, vol. 15, no. 1, pp. 699-713, Jan. 2016.

[11] R. A. Horn and C. R. Johnson, *Matrix Analysis,* 2nd ed. Cambridge, U.K.: Cambridge Univ. Press, 2013.

[12] S. Liu, J. Cheng, and N. C. Beaulieu, "Asymptotic error analysis of diversity schemes on arbitrarily correlated Rayleigh channel," *IEEE Trans. Commun.*, vol. 58, no. 5, pp. 1351-1355, May 2010.

[13] X. Li and J. Cheng, "Asymptotic error rates analysis of selection combining on generalised correlated Nakagami-m channels," *IEEE Trans. Commun.*, vol. 60, no. 7, pp. 1765-1771, July 2012.

[14] M. Z. Win, G. Chrisikos, and J. H. Winters, "MRC Performance for *M*-ary modulation in arbitrarily correlated Nakagami fading channels" *IEEE Commun. Lett.*, vol. 4, no. 10, pp. 301-303, Oct. 2000.

[15] Q. T. Zhang, "Maximal-ratio combining over Nakagami fading channels with an arbitrary branch covariance matrix," *IEEE Trans. Veh. Technol.*, vol. 48, no. 4, pp 1141-1150, July 1999.

[16] P. Lombardo, G. Fedele, and M. M. Rao, "MRC performance for binary signals in Nakagami fading with general branch correlation," *IEEE Trans. Commun.*, vol. 47, no. 1, pp. 44-52, Jan. 1999.